Consequently, the mechanical characteristics of the condition of the metal may not serve as an indicator of its damage by pores.

CONCLUSIONS

1. The process of development of sources of failure in heterogeneous heat-resistant steels is a complex one and may not be described within the limits of any single physical model. More promising is a phenomenological approach to describing the kinetics of this process.

2. The relationship of the damage of the metal by pores to the time of creep is presented and, on the basis of it, a structural method is proposed for determination of the residual life based on the degree of damage by pores.

3. The short-term mechanical properties may not serve as an indicator of the degree of damage of the metal by pores.

LITERATURE CITED

1. V. I. Vladimirov, The Physical Nature of the Fracture of Metals [in Russian], Metallurgiya, Moscow (1984).
2. V. M. Rozenberg, Fundamentals of the High Temperature Strength of Metallic Materials [in Russian], Metallurgiya, Moscow (1973).

RESISTANCE TO DEFORMATION AND FRACTURE OF 35Kh3NM

STEEL UNDER CONDITIONS OF SHOCK LOADING

V. D. Gluzman, G. I. Kanel',   UDC 532.593
V. F. Loskutov, V. E. Fortov,
and I. E. Khorev

1. Formulation of the experiments. Investigations of the strength properties of materials under conditions of shock-wave loading have been stimulated by the necessity of prediction of the action of intense pulsed loads on various structures. Measurements of mechanical properties under these conditions which have been described in the literature have been made primarily on low-strength materials (mild steels, aluminum alloys). In this work the strength properties and features of the $\alpha \rightleftarrows \varepsilon$ structural transformation of high-strength (σ_t = 1.6–1.8 GPa) 35Kh3NM steel were investigated by recording of the wave profiles of the longitudinal stress $\sigma_x(t)$ and the velocity of the free rear surface of the specimens $w(t)$.

The 120-mm-diam. 10–15-mm-thick specimens were cut from a round blank and heat-treated to a hardness of 46–49 HRC. The unidimensional compressive stresses were generated in the specimens by detonation of a 100-mm-diam. shaped explosive charge in direct contact with the specimen or with 2–7-mm-thick aluminum strikers with a diameter of the flat portion at the moment of impact of not less than 60 mm. Impact of the strikers with rates of 0.45–2.0 km/sec was provided with the use of explosive devices.

To record the $w(t)$ profiles capacitive sensors [1] with a measuring electrode diameter of 20 mm and an initial distance between the electrode and the specimen surface of 4–6 mm were used. The $\sigma_x(t)$ profiles of the stresses were recorded with double-wound manganin pressure sensors [2, 3], the dimensions of the sensitive foil elements of which were ∿4.2 × 4.2 mm. The pressure sensors were located between the plates of the composite specimens and insulated with layers of Dacron, fluoroplastic, or mica. The total thickness of the sensors together with the insulation was 0.1–0.2 mm, depending upon the intensity of the shock wave to be recorded.
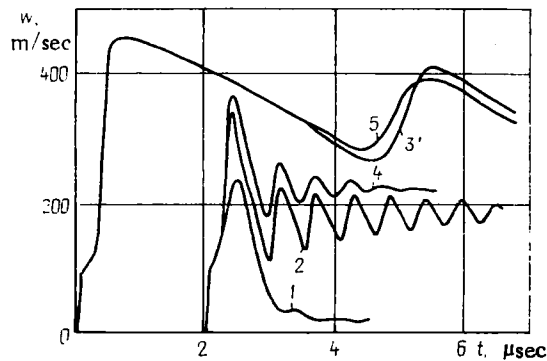
Fig. 1. The results of recording of the pro-
files of the velocity of the free surfaces
of the specimens. (Loading conditions de-
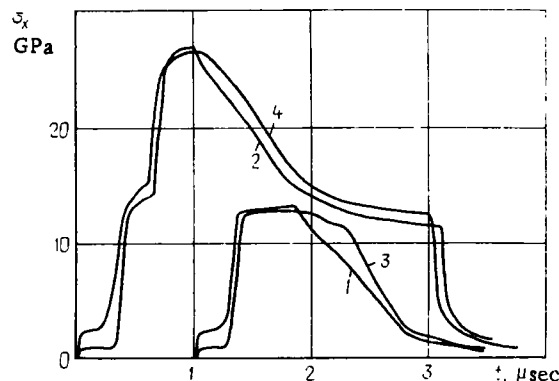scribed in Table 1.)

Fig. 2. Profiles of the stresses in
35Kh3NM steel (curves 1 and 2) and Armco
iron (curves 3 and 4) in loading with
velocities of 2.06 km/sec (upper curves)
and 1.05 km/sec (lower curves): 1) h =
10.7 mm; 2) h = 10.5 mm; 3) h = 9.9 mm;
4) h = 10.1 mm; h) distance from the
surface of the striker to the sensor.

The $w(t)$ profiles of the velocity of the free surface obtained from the tests with
capacitive sensors are shown in Fig. 1. The tests were made both on specimens cut per-
pendicular to the rolling direction (in this case the load was applied in the rolling
direction) and on specimens the planes of which coincided with the rolling direction. On
the $w(t)$ profiles were recorded the exit on the surface of the elastoplastic compression
wave and of the head portion of the low-pressure wave and, in tests with a sufficiently
large amplitude of the original wave, the split-off pulse, revealed in separation of the
internal layers of the specimen.

Figure 2 shows the $\sigma_x(t)$ profiles of stresses in 35Kh3NM steel and in Armco iron ob-
tained in tests with manganin sensors. The multiwave structure with splitting of the plas-
tic shock wave and the formation of a low-pressure shock wave in the tests with the maximum
load is related to the reversible $\alpha \rightleftarrows \epsilon$ polymorphic transformation in iron and steel.

2. The split-off strength of steel. With a striker velocity of 450 m/sec the $w(t)$
profile practically duplicates the form of the compression pulse within the specimen (curve
1 in Fig. 1). The low residual velocity in the "tail" of the pulse is determined by the
hysteresis of the elastoplastic deformation in the compression—tension cycle [4]. The re-
flection of the compression pulse from the free surface of the solid body is accompanied by
a change in sign of the load [5]. With an increase in the amplitude of the original com-
pression pulse, the amount of the tensile stresses generated increases all the way to the
start of failure (splitting-off). Failure leads to unloading of the material in tension
and the appearance of a compression wave exiting to the surface in the form of a "split-

TABLE 1. The Results of Measurements of the Split-Off Strength

Curve in Fig. 1	Orientation of the load relative to the rolling direction	Loading conditions	Specimen thickness, mm	w^{max}, m/sec	δ, mm	$\dot{w}_1 \cdot 10^6$, m/sec²	$\dot{w}_2 \cdot 10^6$, m/sec²	Δw, m/sec	σ^*, GPa
1	Parallel	Impact of a 2-mm-thick aluminum plate with a velocity of v=450±15 m/sec	10.1	207±5	—			177±10	—
2	»	The same, v=700±30 m/sec	10.4	338±5	1.6	500±50	1250	221±10	4.4±0.2
3	»	Detonation of a shaped explosive charge in contact with the specimen	15.2	456±5	9.9	74±7	273	194±10	4.0±0.2
4	Perpendicular	Impact of a 2-mm thick aluminum plate with a velocity of v=700±30 m/sec	9.8	368±5	1.5	500±50	750	192±5	3.85±0.1
5	»	Detonation of a shaped explosive charge in contact with the specimen	15.0	456±5	9.4	60	150	170±10	3.4±0.2

off pulse" (curves 2-5 in Fig. 1). Subsequently repeated reflections of the split-off pulse between the rear surface of the specimen and the surface of the fracture cause vibrations in the recorded velocity w(t) with a period of Δt equal to double the time of passage of the disturbance through the split-off plate: $\Delta t = 2\delta/c_e$, where δ is the thickness of the split-off plate and $c_e = 5.90 \pm 0.05$ km/sec, the "longitudinal" speed of sound.

From a comparison of profiles 2 and 4 in Fig. 1 it may be seen that damping of the oscillations in the velocity in tests with a loading direction perpendicular to the rolling direction occurs more rapidly than in the tests with orientation of the load parallel to rolling. This correlates with the form of the fracture surfaces. In the transverse-cut specimens, the fracture surface was quite uniform with a primary height of the irregularities of significantly less than 0.1 mm. With orientation of the load perpendicular to the rolling direction, the fracture surface was much rougher, with a clearly visible texture. It is obvious that reflection of a short pulse from a nonuniform surface must be accompanied by dispersion of it and accelerated damping.

The values of the failure stresses σ^* were determined from the difference Δw between the maximum value of w and the value of w in advance of the front of the split-off pulse [6]:

$$\sigma^* = \frac{1}{2} \rho_0 c_0 (\Delta w + \delta w),$$

where $\rho_0 = 7.76$ g/cm³ is the density of the material and $c_0 = 4.65$ km/sec, the "three-dimensional" speed of sound, taken as equal to that measured for Armco iron [7]. For steels of different composition, the three-dimensional speed of sound differs little from this value [8].

The introduction of the correlation δw is related to the difference in the rates of the unloading portion of the original compression wave and of the front of the split-off pulse [9]. Taking into consideration the steepness of the split-off pulse, this correction is determined as

$$\delta w = (\delta/c_0 - \delta/c_e) \frac{\dot{w}_1 \dot{w}_2}{\dot{w}_1 + \dot{w}_2},$$

where $\dot{w}_1$ and $\dot{w}_2$ are the absolute values of the accelerations in the incident low-pressure wave and in the split-off pulse.

The values of the split-off strength and the experimental data used in finding them are given in Table 1. It may be seen that in the tests with a short loading pulse the failure stresses are 10% higher than with a long pulse. With orientation of the load perpendicular to the rolling direction, the split-off strength of the steel is about 15% lower than in loading in the rolling direction. In the latter case, steeper split-off pulses are observed, which is related to the greater localization of fracture. The values of the split-off strength for 35Kh3NM steel are more than twice as high as for Armco iron [10].

3. The elastoplastic properties of the steel. 35Kh3NM steel is characterizied by significant strain hardening. Its influence on the shock-wave compression process is graphically demonstrated by the results of tests with capacitative sensors possessing, as the result of contact-free measurements, good resolving capacity with respect to time.

As may be seen from the profiles presented in Fig. 1, the compression waves consist of an elastic jump in which a velocity of the surface of $w_e = 95 \pm 5$ m/sec is reached, a plastic shock wave, and an area of a smooth increase in velocity between the elastic and plastic waves. In the elastic jump, the longitudinal stress increases to a value of $\sigma_x = \frac{1}{2}\rho_0 c_e w_e = 2.2 \pm 0.1$ GPa, which corresponds to a maximum shear stress of $\tau = \frac{3}{4}\sigma_x(1-K/E')=0.62\pm0.03$ GPa, where $K = \rho_0 c_0^2$ is the modulus of all-sided compression and $E' = \rho_0 c_e^2$ is the modulus of longitudinal elasticity. Within the limits of measurement error, the amplitude of the elastic jump depends neither upon the intensity of the shock wave nor upon the distance passed, which provides a basis for assuming that the increase in the parameters in the transition area between the elastic and the plastic waves is determined primarily by strain hardening and not by viscous effects. The hardening may be determined qualitatively.

If the structure of the transition area is determined only by strain hardening, then the compression wave may be considered as a simple wave for which $d\sigma_x = -\rho_0^2 c_\sigma^2 dV$, where c_σ is the Lagrange phase velocity in the wave. Here and subsequently we will assume as positive the compressive stress and deformation. In uniaxial deformation, the increase in plastic deformation is

$$d\gamma = -\frac{dV}{V} - \frac{d\tau}{G} \ ,$$

where G is the shear modulus.

Assuming that $d\tau = \frac{3}{4}\left(1 - \frac{c_0^2}{c_\sigma^2}\right)d\sigma_x$, we obtain:

$$\frac{d\gamma}{d\tau} = -\frac{1}{V}\cdot\frac{dV}{d\sigma_x}\cdot\frac{d\sigma_x}{d\tau} - \frac{1}{G} = \frac{4}{3\rho_0(c_\sigma^2 - c_0^2)} - \frac{1}{G} \ ;$$

$$\frac{d^2\gamma}{d\tau^2} = -\frac{8}{3\rho_0}\cdot\frac{c_\sigma}{(c_\sigma^2 - c_0^2)^2}\frac{dc_\sigma}{d\sigma_x}\cdot\frac{d\sigma_x}{d\tau} = -\frac{32}{9\rho_0}\cdot\frac{c_\sigma^3}{(c_\sigma^2 - c_0^2)^3}\cdot\frac{dc_\sigma}{d\sigma_x} \ . \tag{1}$$

Using the rule of hardening in the form

$$\tau = \tau_0 + A\gamma^{1/2}, \tag{2}$$

we have:

$$\frac{d^2\gamma}{d\tau^2} = 2/A^2. \tag{3}$$

Equating Eqs. (1) and (3), we obtain the expression for finding the hardening constant A:

$$A^2 = -\frac{9(c_\sigma^2 - c_0^2)^3 \rho_0}{16 c_\sigma^3 dc_\sigma/d\sigma_x} \ . \tag{4}$$

As a first approximation for determination of the value of $dc_\sigma/d\sigma_x$, it is possible to use the rule of doubling of the mass velocity in reflection of a compression wave from a free surface:

$$\frac{dc_\sigma}{d\sigma_x} = \frac{dc_\sigma}{dw}\cdot\frac{dw}{d\sigma_x} = \frac{dc_\sigma}{dw}\cdot\frac{2}{\rho_0 c_\sigma} \ .$$

The phase velocity c_σ is determined as a first approximation as

$$c_\sigma = \frac{h}{h/c_e + \Delta t(w)} \ ; \qquad \frac{dc_\sigma}{dw} = -\frac{c_\sigma^2}{h}/\dot{w},$$

where h is the specimen thickness and $\dot{w}$ is the steepness of the experimental w(t) profile after the period of time Δt after exit to the surface of the front of the elastic forerunner.

Therefore

$$\frac{dc_\sigma}{d\sigma_x} = -\frac{2c_\sigma}{\rho_0 h\dot{w}} \ . \tag{5}$$

A more detailed analysis taking into consideration the interaction of the incident and reflected waves gives
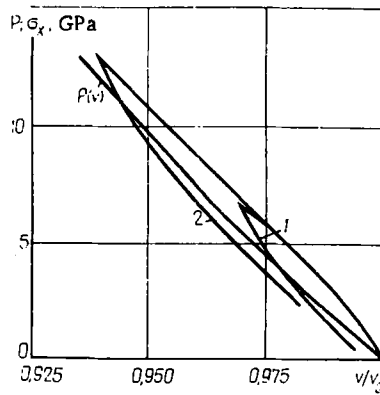
Fig. 3. Trajectories of the change in condition of the steel in compression pulses: 1, 2) $\sigma_x(V)$ relationships obtained from experiments with amplitudes of the load pulses of 6.5 and 13.2 GPa, respectively ($p(V)$ — curve of all-sided compression of iron [7]).
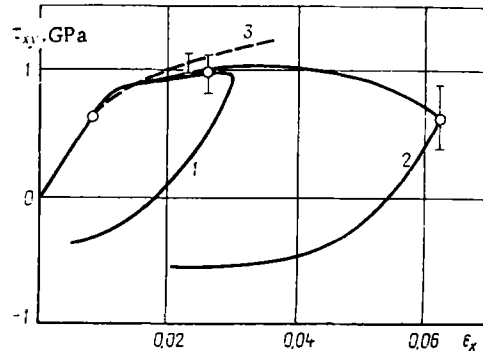

Fig. 4. 1, 2) Shear stress τ—deformation ε curves for load pulses with amplitudes of 6.5 and 13.2 GPa, respectively; 3) hardening curve calculated according to Eq. (7).

$$c_\sigma = c_e \frac{2h - c_e \Delta t}{2h + c_e \Delta t} \ ; \qquad \frac{d\sigma}{dw} = \rho_0 \frac{c_\sigma c_e (c_e + c_\sigma)}{c_e (c_e + c_\sigma) + 2c_\sigma^2} \ ;$$

$$\frac{dc_\sigma}{d\sigma_x} = - \frac{c_e^2 + c_e c_\sigma + 2c_\sigma^2}{\rho_0 \dot{w} c_\sigma (2h + c_e \Delta t)} \ . \tag{6}$$

With $c_\sigma = c_e$ Eqs. (5) and (6) are equivalent. For the center portion of the transition area with $h = 10$ mm, $c_\sigma = 5.32$ km/sec, $\dot{w} = (3 \pm 0.3) \cdot 10^8$ m/sec², and $\Delta t = 0.2$ μsec after substitution of Eq. (6) in Eq. (4), we obtain $A = 4.3 \pm 1$ GPa (taking into consideration the indeterminacy of c_e, c_0 and c_σ). The use of Eq. (5) in Eq. (4) gives values of A too high by 10%. Therefore, in the initial stage of dynamic deformation, the fatigue curve of 35Kh3NM steel is described by the relationship

$$\tau = (0.62 + 4.3\sqrt{\gamma}), \ \text{GPa} \tag{7}$$

Information on the resistance of the material to further deformation in the compression pulse may be obtained from an analysis of the full $\sigma_x(t)$ stress profiles. For this purpose, three series of tests were made with loading of the specimens by aluminum strikers with a thickness of 5 mm at a velocity of 590 ± 10 m/sec, with a thickness of 4 mm at a velocity of 1.05 ± 0.05 km/sec, and with a thickness of 7 mm at 2.0 ± 0.05 km/sec.

As may be seen from the experimental $\sigma_x(t)$ profiles presented in Fig. 2, a clear separation of the elastic forerunners in the low-pressure waves is observed neither in steel nor in iron. A comparison of the stress profiles indicates that deformation of the stronger steel is associated with higher deviator stresses than in the case of iron in the whole shock compression and unloading cycle. Apparently, the increased resistance of the steel leads to an increase in comparison with iron in the apparent hysteresis of forward and reverse polymorphic transformations. Probably the boundaries of stability of the phases are determined by their density or effective pressure but not by the normal stress.

From the stress profiles obtained it is possible, in approximation of a simple wave, to determine the trajectories of the change in condition in stress σ_x–specific volume V coordinates:

$$\frac{V - V_0}{V_0} = -\int_0^{\sigma_x} \frac{d\sigma_x}{\rho_0 c_\sigma^2 (\sigma_x)} .$$

The Lagrange speeds of sound c_σ were determined either directly from the results of recording of the $\sigma_x(t)$ profiles in two cross sections of the specimen, as from tests with $\sigma_x^{max} = 6.6$ MPa, or by "comparison with a standard." The latter method is based on comparison of the stress profiles in the investigated and some standard material. If the distance from the surface of the striker to the cross section of the specimen of the investigated material measured by the sensor is equal to x_0 and the same for the standard is equal to x_s and the Lagrange speed of propagation of the portion of the wave with the stress σ_x in the standard material is equal to c_s, then

$$c_\sigma (\sigma_x) = \frac{x_0 c_s (\sigma_x)}{c_s (\sigma_x)(t_0 - t_s) + x_s} ,$$

where $t_0 - t_s$ is the difference between the moments of arrival on the sensor of the area of the wave with the stress σ_x in the specimen and in the standard material. The results of tests with iron [3] and aluminum [11] were used as the standard stress profiles.

The trajectories of the change in condition of the steel constructed from the experimental data are shown in Fig. 3. It also shows the p(V) all-sided compression curve, for which the shock adiabatic curve obtained in [7] with deduction of the deviator component of stresses was used. The maximum shear stresses were determined from the deviation of the trajectory of the change in condition from the curve of all-sided compression:

$$\tau = \frac{3}{4} (\sigma_x (V) - p (V)).$$

The deformation under the given loading conditions is determined as

$$\varepsilon_x = -\int_{V_0}^{V} \frac{dV}{V} = -\ln \frac{V}{V_0} .$$

The deformation curves obtained in this manner are shown in Fig. 4. It also shows the hardening curve calculated using Eq. (7). It may be seen that, with an increase in the amplitude of the shock wave, the stressed condition behind its front deviates from that described by Eq. (7) and approaches isotropic. The deformation curves demonstrate the presence of a significant Bauschinger effect.

Qualitatively, the stress profiles in the unloading portion correspond to that expected for viscoelastic materials. From the determination of the rate of deformation, it follows that the intrinsic viscosity in the given case is 10^4 Pa·sec.

The rates of propagation of the low-pressure wave front in elastoplastic materials are equal to the longitudinal speed of sound. Taking into consideration the degree of compression, they are 6.3 km/sec with $\sigma_x^{max} = 6.5$ GPa, 6.54 km/sec with $\sigma_x^{max} = 13.2$ GPa, and 6.75 km/sec with $\sigma_x^{max} = 26.7$ GPa. Before the start of the polymorphic transformation, the relationship of the longitudinal speed of sound to pressure with an accuracy no poorer than ±1.5% is described, assuming constancy of Poisson's ratio.

LITERATURE CITED

1. A. G. Ivanov and S. A. Novikov, "A capacitive sensor method for recording the instantaneous speed of a moving surface," Prib. Tekh. Eksp., No. 1, 135-138 (1963).

2. G. I. Kanel', The Use of Manganin Sensors for Measuring the Shock Compression Pressures of Condensed Media [in Russian], Moscow (1974), Manuscript deposited in the All-Union Institute for Scientific and Technical Information, No. 477-74 Dep.
3. A. V. Anan'in, A. I. Dremin, and G. I. Kanel', "Polymorphic transformations of iron in a shock wave," Fiz. Goreniya Vzryva, No. 3, 93-102 (1981).
4. G. I. Kanel' and É. N. Petrova, "The strength of VT6 titanium under conditions of shock-wave loading," in: Detonation: Materials of the Second All-Union Conference on Detonation, Chernogolovka (1981), pp. 136-142.
5. Ya. B. Zel'dovich and Yu. P. Raizer, Physics of Shock Waves and High-Temperature Hydrodynamic Phenomena, Academic Press.
6. S. A. Novikov, I. I. Divnov, and A. G. Ivanov, "An investigation of the fracture of steel, aluminum, and copper in explosive loading," Fiz. Met. Metalloved., 21, No. 4, 608-615 (1966).
7. L. M. Barker and R. E. Holleenbach, "Shock wave study of the phase transition in iron," J. Appl. Phys., 45, No. 11, 4872-4887 (1974).
8. W. H. Gust, D. J. Steinberg, and D. A. Young, "Hugoniot parameters to 320 GPa for three types of steel," High-Temp.—High Pressures, 11, No. 3, 271-280 (1979).
9. G. V. Stepanov, "The split-off fracture of metals by plane elastoplastic loading waves," Probl. Prochn., No. 8, 66-70 (1976).
10. G. I. Kanel', "The resistance of metals to split-off fracture," Fiz. Goreniya Vzryva, No. 3, 77-83 (1982).
11. A. N. Dremin, G. I. Kanel', and O. B. Chernikova, "The resistance to plastic deformation of AD1 aluminum and D16 duralumin under conditions of shock compression," Zh. Prikl. Mekh. Tekh. Fiz., No. 4, 132-138 (1981).

CHANGE IN THE DUCTILITY CHARACTERISTICS OF AUSTENITIC

STEELS DURING DEFORMATION AT DIFFERENT RATES

E. T. Shinkarenko

UDC 620.17:669.14

It is widely believed that an increase in strain rate leads to an increase in ductility. This is indicated, for example, by the data in [1, 2].

The results of other authors make it possible to suggest that the ductility of steels decreases in the transition from static deformation to dynamic straining [3-6].

The present study investigates the ductility of stable austenitic steels 07Kh13AG19N5 and 12Kh18N22T and metastable austenitic steel 03Kh13AG19.

Aften an austenizing quenching (6- and 7-point grain size), the steels were tested in tension at 20 and −196°C at strain rates from $1.7 \cdot 10^{-4}$ sec^{-1} to $5 \cdot 10^{2}$ sec^{-1}.

The ductility of the steels was evaluated from the quantities ε_ψ and ε_{ψ_p}, which were found from the equations

$$\varepsilon_\psi = \ln \frac{1}{1-\psi}; \qquad \varepsilon_{\psi_p} = \frac{1}{1-\psi_p} \quad [4],$$

where ε_ψ is the total plastic strain (true strain after fracture); ψ is the reduction of area of the specimen after fracture; ε_{ψ_p} is the uniform plastic strain (true strain at the moment necking begins); ψ_p is the reduction of area of the specimen at the moment necking begins.

It was established from the study that the ductility of the structurally stable steels is reduced by a transition from static deformation to dynamic deformation at 20°C (Figs. 1 and 2).

There is a similar change in the ductility of steel 03Kh13AG19 under these conditions. with the $\gamma \to \varepsilon$-transformation occurring in this steel during deformation at rates $\dot\varepsilon < 10^{-1}$ sec^{-1} [5].